

Characterization of tumor microenvironment and cell interaction patterns in testicular and diffuse large B-cell lymphomas

Matias Autio,¹⁻³ Oscar Brück,^{4,5} Marjukka Pollari,^{1,3,6} Marja-Liisa Karjalainen-Lindsberg,⁷ Klaus Beiske,⁸ Judit Mészáros Jørgensen,⁹ Harald Holte,¹⁰ Teijo Pellinen,¹¹ Suvi-Katri Leivonen¹⁻³ and Sirpa Leppä¹⁻³

¹Research Programs Unit, Applied Tumor Genomics, University of Helsinki, Helsinki, Finland;

²Department of Oncology, University of Helsinki and Helsinki University Hospital

Comprehensive Cancer Center, Helsinki, Finland; ³iCAN Digital Precision Medicine Flagship,

Helsinki, Finland; ⁴Hematoscope Lab, Comprehensive Cancer Center & Center of

Diagnostics, Helsinki University Hospital, Helsinki, Finland; ⁵Department of Oncology,

University of Helsinki, Helsinki, Finland; ⁶Department of Oncology, Tampere University

Hospital, Tampere, Finland; ⁷Department of Pathology, Helsinki University Hospital, Helsinki,

Finland; ⁸Department of Pathology, Oslo University Hospital, Oslo, Norway; ⁹Department of

Hematology, Aarhus University Hospital, Aarhus, Denmark; ¹⁰Department of Oncology, and

KG Jebsen Centre for B Cell Malignancies, Oslo University Hospital, Oslo, Norway and

¹¹Institute for Molecular Medicine Finland (FIMM), Helsinki, Finland


Correspondence: S. Leppä
sirpa.leppa@helsinki.fi

Received: July 12, 2024.

Accepted: December 2, 2024.

Early view: December 12, 2024.

<https://doi.org/10.3324/haematol.2024.286267>

Published under a CC BY license 

Abstract

The tumor microenvironments (TME) of diffuse large B-cell lymphoma (DLBCL) subgroups have remained poorly characterized. Here, we dissected the composition and spatial organization of the TME in germinal center B-cell (GCB), activated B-cell (ABC), and testicular (T-) DLBCL using gene expression profiling and multiplex immunohistochemistry. We found that high proportions of M2-like tumor-associated macrophages (TAM) and cytotoxic tumor-infiltrating T cells (TIL) were characteristic of ABC DLBCL TME. Furthermore, high CD8⁺ TIL content translated to favorable outcomes. In contrast, GCB DLBCL TME was enriched in CD4⁺ TIL, regulatory TIL, and a higher M1-like : M2-like TAM ratio, and high proportions of TAM and Granzyme B⁺ cells associated with worse survival. TIL and TAM interacted more frequently with M2-like TAM and cytotoxic TIL in the ABC DLBCL in contrast to GCB subtype, where the interactions were more abundant with other TIL and CD4⁺ TIL. In T-DLBCL, TME resembled that of ABC DLBCL with a higher proportion of M2-like TAM and cytotoxic cells, except that checkpoint-positive TIL were less prominent compared to DLBCL NOS. Cytotoxic TIL also interacted more with TIL and TAM. A large number of CD163⁺ TAM interactions with distinct TIL translated to unfavorable survival both in GCB DLBCL and T-DLBCL, whereas a high number of interactions between TIL and TAM, CD4⁺ TIL and TAM, and CD4⁺ TIL and other TIL were associated with favorable outcomes only in T-DLBCL. Together, our data demonstrate biologically and clinically relevant differences in the composition of and cellular interactions in the TME between various DLBCL entities.

Introduction

The tumor microenvironment (TME) of diffuse large B-cell lymphoma, not otherwise specified (DLBCL, NOS), is heterogeneous. It consists of blood vessels, extracellular matrix, stromal cells, and variable proportions of immune cells, including T lymphocytes, macrophages, and natural killer (NK) cells reacting to the emergence of pathogenic lymphocytes.^{1,2} However, TME can also promote lymphoma growth by offering pro-tumorigenic signals and a protective milieu to lymphoma cells.³ Based on gene expression pro-

files reflecting differences in the composition of the TME, novel DLBCL subtypes with distinct biological features and outcomes have recently been proposed.^{4,5} Likewise, clinical associations of distinct tumor infiltrating immune cell phenotypes, including checkpoint molecule-expressing T lymphocytes and macrophages have also been discovered and the spatial organization of the TME has also been uncovered.⁶⁻¹⁴ To date, however, different TME-targeted therapies, such as PD-1 blockade have not shown any clinically significant efficacy in DLBCL, and further characterization of factors predictive for outcome is warranted.¹⁵

Based on the cell-of-origin (COO), DLBCL NOS (DLBCL) is divided into germinal center B-cell (GCB)-like and activated B-cell (ABC)-like molecular subtypes.¹⁶ The subtypes differ clinically, with GCB DLBCL having a higher sensitivity to first-line treatment consisting of rituximab, cyclophosphamide, doxorubicin, vincristine, and prednisone (R-CHOP).^{17,18} Biologically, they harbor different genetic aberrations reflecting different pathogenesis.^{19,20} While GCB DLBCL originates from GCB cells with frequent alterations in genes, such as *BCL2* and *EZH2*, ABC DLBCL is derived from more mature, post-GC B cells; it is characterized by continual activity of the NF- κ B pathway.^{21–23} Based on genetic aberrations, DLBCL can also be divided into distinct genetic subgroups.^{24,25} Testicular diffuse large B-cell lymphoma (T-DLBCL) is a rare lymphoid malignancy of the testes, most commonly arising among elderly males.²⁶ On a molecular level, most cases represent ABC DLBCL, and in the advanced stage, they are at high risk of recurrence and have a dismal prognosis.²⁷ We have previously shown that, based on the TME composition, DLBCL can be classified into inflamed and non-inflamed subtypes.^{11,12} While the inflamed subtype is associated with favorable outcome in T-DLBCL,²⁸ immune checkpoint expression in T cells and low T-cell/macrophage proportion translates to inferior outcome in DLBCL NOS.^{11,12} Despite the evidence of its clinical significance, differences in the composition and spatial organization of the TME between GCB, ABC, and T-DLBCL have been poorly characterized. We hypothesized that the differences in the pathogenesis, biology, and clinical outcome of these subtypes are reflected in the TME. Here, we compare the TME composition and cell interaction patterns between these subtypes, and how they associate with survival.

Methods

Patients and samples

Study populations are presented in *Online Supplementary Table S1*. The DLBCL gene expression cohort consisted of 69 patients treated in the Nordic LBC-05 and LBC-04 trials,^{29,30} whereas T-DLBCL gene expression, DLBCL multiplex immunohistochemistry (mIHC), and T-DLBCL mIHC cohorts consisted of 60, 175, and 80 retrospectively collected patients, respectively. Thirty-four DLBCL patients and 60 T-DLBCL patients overlapped between the gene expression and mIHC cohorts. Patients with high-grade B-cell lymphoma were excluded. We constructed tumor microarrays (TMA) from formalin-fixed paraffin-embedded (FFPE) primary diagnostic tumor tissue.³¹ We also used gene expression data of 496 DLBCL patients from the Reddy et al. (EGAS00001002606) and 562 DLBCL patients from the Schmitz et al. cohorts.^{24,32}

The study was approved by the Ethics Committee of Helsinki University Hospital, Finland, the Finnish National Authority for Medicolegal Affairs (VALVIRA), and the Institutional Re-

view Board. The patients treated in Nordic phase II studies LBC-04 and LBC-05 signed an informed consent before study enrollment. Sample collection was performed according to the principles of the Declaration of Helsinki. Trials were registered at clinicaltrials.gov (identifiers 01502982 and 01325194).

Gene expression profiling

We used Nanostring gene expression data performed on primary diagnostic FFPE tumor tissue using a Nanostring nCounter Human PanCancer Immunoprofiling Panel (XT-CSO-HIP1-12, Nanostring Technologies, Seattle, WA, USA).^{11,28} Molecular subtypes determined with DLBCL90 assay (NanoString) were available for 47/69 patients (68%) in the DLBCL gene expression cohort. For the DLBCL mIHC cohort, COO was available for 137 patients (78%) based on RNA sequencing (N=101) and Lymph2Cx assay (N=36).^{33,34}

Immunohistochemistry and cell-to-cell interaction analyses

We used mIHC data performed on TMA constructed from diagnostic FFPE tumor tissue of 175 patients with primary DLBCL and 80 patients with primary T-DLBCL.^{11,12,35} We characterized T cells, macrophages, NK cells, B cells, and immune checkpoint molecules (*Online Supplementary Table S2*). All mIHC panels are described in detail in the *Online Supplementary Methods*. We filtered out areas with staining artifacts using Ilastik v.1.3.3 software and performed automated digital quantification using CellProfiler v.3.1.8 software (<https://cellprofiler.org/>).^{36,37} We had previously performed IHC stainings for β_2 microglobulin (B2M), HLA-ABC, and HLA-DR.^{11,28}

Cell-to-cell interaction analyses were performed on 229 mIHC stained samples, using the method developed by Brück et al.³⁸ We defined cells with a Euclidean distance <100 pixels (22 μ m) from each other as interacting cells.³⁹ We calculated an interaction index based on the number of cell-to-cell interactions normalized to the number of corresponding cell types in each sample. More details are provided in the *Online Supplementary Methods*.

Statistical analyses

We performed all statistical analyses using R v.4.1.2. For unsupervised hierarchical clustering analyses we used Euclidean distance and Ward's linkage. We used univariable and multivariable Cox proportional hazards regression models to estimate the prognostic significance of each variable, and the Kaplan-Meier method with log-rank test to estimate the difference in survival between patient groups. We defined overall survival (OS) as the time from diagnosis to death from any cause and progression-free survival (PFS) as the time from diagnosis to progression or death from any cause. We used Mann-Whitney U and Kruskal-Wallis H tests to compare two or more groups, respectively. The Benjamini-Hochberg method was used

to correct *P* values for errors caused by multiple testing.

Results

Patients’ characteristics

Patients’ characteristics of the five study cohorts are presented in the *Online Supplementary Table S1*. The DLBCL gene expression cohort consisted of 69 patients. Median age was 55 years (range 22-65), and disease characteristics were typical of high-risk DLBCL.¹¹ Median follow-up time was 65 months (interquartile range (IQR): [51 months; 68 months]), during which 11 patients relapsed and 9 died, translating to 86% and 88% 5-year PFS and OS rates. Twenty-four (35%) patients had GCB DLBCL, 16 (23%) had ABC DLBCL, and 7 (10%) remained unclassified. In 22 (32%) cases, data on the COO was unavailable. Five-year OS rates for the patients with GCB and ABC DLBCL were 95.8% and 87.5% (*P*=0.300), respectively.

The DLBCL mIHC cohort consisted of 175 patients with a median age of 61 years (range: 16-84). During a median follow-up time of 62 months (IQR: 44 months; 68 months), 28 patients relapsed and 33 died, translating to 76% PFS and 79% OS at 5 years.¹² Sixty-one (35%) patients had GCB DLBCL, 58 (33%) had ABC DLBCL, and 18 (10%) were unclassified. In 38 (22%) cases, data on COO were unavailable. Five-year OS rates for the patients with GCB DLBCL and ABC DLBCL were 92.9% and 64.6% (*P*<0.001), respectively.

The T-DLBCL gene expression and mIHC cohorts consisted of 60 and 80 patients, with a median age of 69 years (range 36-83) and 70 years (range 36-92).^{28,35} As is typical

for T-DLBCL, most patients (40/60 [67%] in the gene expression cohort and 56/80 [70%] in the mIHC cohort) had non-GC DLBCL. In the gene expression cohort, the median follow-up time was 76 months (IQR: 54 months; 134 months), during which 27 patients relapsed or died, and in the mIHC cohort, 76 months (IQR: 53 months; 133 months), during which 41 patients relapsed or died. Five-year OS rates were 60.1% in the gene expression cohort and 53.6% in the mIHC cohort.

Expression of immune-related genes in the germinal center B-cell-like and activated B-cell-like diffuse large B-cell lymphoma

To get an overview of the immunological landscape of GCB and ABC DLBCL, we first analyzed the differential expression of immune-related genes using a Nanostring nCounter platform. As expected, ABC DLBCL expressed high levels of ABC markers, such as *TNFRSF13B* and *IRF4*, but also genes related to macrophage signaling, such as *CD163* and *CD47*. In comparison, GCB DLBCL over-expressed genes related to T-cell receptor signaling, such as *ICOSLG*, *HLA-DOB*, *IL4*, and *CD40LG* (Figure 1A and *Online Supplementary Table S3*). Furthermore, using unsupervised hierarchical clustering, we could accurately separate GCB and ABC subtypes based on the expression of these most differentially expressed immune-related genes (adjusted [adj.] *P*<0.01) (Figure 1B). To validate our findings, we used RNA-seq data from 496 DLBCL from the Reddy et al. cohort and 562 DLBCL from the Schmitz et al. cohort.^{24,32} By analyzing the same gene set as in the Nanostring cohort, we found that many of the previously identified genes were differentially expressed

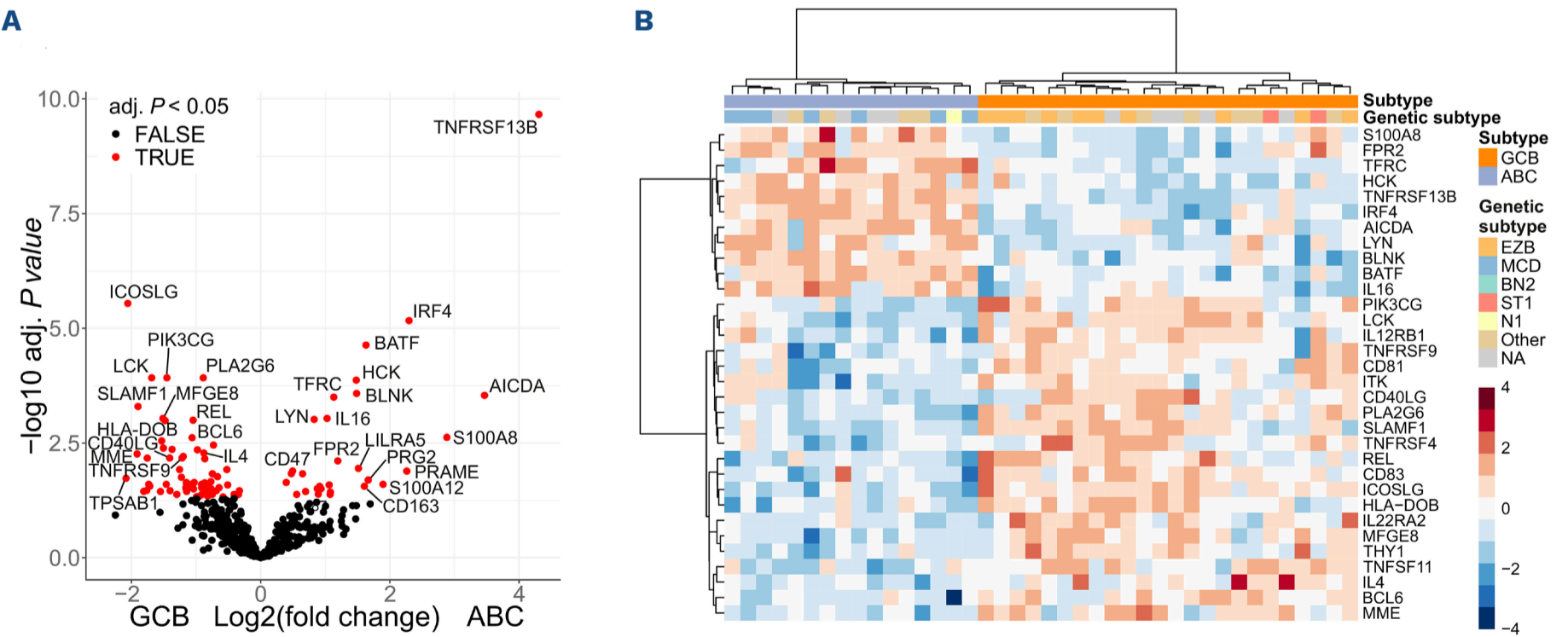


Figure 1. Differentially expressed immune-related genes between germinal center B-cell-like and activated B-cell-like diffuse large B-cell lymphoma. (A) Volcano plot depicting differentially expressed immune-related genes between activated B-cell like (ABC) and germinal center B-cell-like (GCB) diffuse large B-cell lymphoma (DLBCL) in the DLBCL, not otherwise specified (NOS) gene expression cohort. (B) Unsupervised hierarchical clustering of patients in the DLBCL, NOS gene expression cohort based on the expression of the 32 most differentially expressed genes (adjusted [adj.] *P*<0.01) between ABC and GCB DLBCL.

also in the validation cohorts (*Online Supplementary Table S4* and *Online Supplementary Figures S1A, S2A*). Analogously, clustering of the most differentially expressed immune-related genes separated GCB and ABC subtypes (*Online Supplementary Figures S1B, S2B*). Likewise, genes associated with macrophage signaling, such as *CD163*, and cytotoxicity, such as *GZMB*, *GZMH*, *GZMM*, and *PRF1*, were over-expressed in the ABC subtype in the Reddy et al. cohort (adj. $P < 0.001$ for all) (*Online Supplementary Figure S1C-P*). Instead, we did not observe any significant differences in the expression of *CD3*, *CD4*, or *CD8* T-cell genes (*Online Supplementary Figure S1H-L*).

The composition of the tumor microenvironment differs between germinal center B-cell-like and activated B-cell-like diffuse large B-cell lymphoma

Next, we studied the composition of the TME at the cellular level using mIHC in 175 DLBCL NOS samples (Figure 2A). Comparing the TME compositions between GCB and ABC subtypes, we found that *CD163*⁺ tumor-associated macrophages (TAM) were enriched in the ABC subtype (median: 11.9% vs. 3.84%; adj. $P < 0.001$), whereas in the GCB subtype, a higher proportion of all TAM were *CD163* negative (median: 79.2% vs. 52.0%; adj. $P < 0.001$) (Figure 2B-D and *Online Supplementary Table S5*). When we analyzed tumor-infiltrating T lymphocytes (TIL), we did not observe significant differences in the proportion of TIL as such between the two molecular subtypes (median: ABC 14.5% vs. GCB 13.9%; adj. $P = 0.448$) (*Online Supplementary Figure S3A-C*). However, in the GCB subtype, a higher proportion of TIL were *CD4*⁺ T-helper cells (median: 66.1% vs. 55.8%; adj. $P = 0.023$) and regulatory T cells (Tregs) (median: 8.66% vs. 5.26%; adj. $P = 0.015$), whereas in the ABC subtype, a higher proportion of TIL were Granzyme B⁺ (GrB⁺) (median: 1.02% vs. 0.39%; adj. $P = 0.008$) (Figure 2E-G). In addition, GrB⁺ cytotoxic cells as such were more abundant in the ABC subtype (median: 0.38% vs. 0.14%; adj. $P = 0.002$) (*Online Supplementary Figure S3D*). Interestingly, the proportion of immune checkpoint-expressing cells also differed according to the subtype, PD-L1⁺ *CD163*⁺ TAM being more frequent in ABC DLBCL (median: 0.74% vs. 0.10%; adj. $P = 0.001$) (Figure 2H and *Online Supplementary Figure S3E-I*). Finally, the presence of immune cells altogether tended to be higher in the TME of ABC DLBCL, as analyzed by the number of *CD20* negative cells, although statistical significance was not reached (median: 42.2% vs. 35.0%; adj. $P = 0.065$) (*Online Supplementary Figure S3J*).

Next, we examined whether HLA and B2M expression differs between GCB and ABC DLBCL. We observed higher expression of HLA-ABC and B2M in the ABC subtype compared to the GCB subtype (HLA-ABC⁺ 67% vs. 32%; $P < 0.001$; B2M⁺ 37% vs. 12%; $P = 0.005$). However, there was no difference in HLA-DR positivity between the subtypes ($P = 0.835$) (*Online Supplementary Figure S3K*). Furthermore, neither the proportion of HLA-ABC nor B2M correlated with the proportion

of TIL or TAM (*Online Supplementary Figure S4*).

The tumor microenvironment of testicular diffuse large B-cell lymphoma compared to diffuse large B-cell lymphoma, not otherwise specified

We wanted to extend our analyses to T-DLBCL, which typically are of ABC origin, and to explore whether T-DLBCL resembled ABC DLBCL in their TME composition. However, in a principal component analysis (PCA) based on the expression of immune-related genes in 60 T-DLBCL and 69 DLBCL NOS samples, T-DLBCL were separated from the DLBCL samples (Figure 3A). Similarly, in an unsupervised hierarchical clustering including all immune-related genes, T-DLBCL and DLBCL cases formed separate clusters, except for one ABC DLBCL, which clustered with T-DLBCL (*Online Supplementary Figure S5A*). Particularly genes related to cell division, such as *CDK1*, *BIRC5*, and *PRKCE*, and genes related to B-cell receptor signaling, such as *BCL2*, *CD79B*, *NFKB1*, and *BLNK* were up-regulated, whereas genes related to antigen presentation and processing and T-cell activation, including many HLA genes, were down-regulated in T-DLBCL compared to DLBCL (*Online Supplementary Table S6* and *Online Supplementary Figure S5B*). The results show that clinical subtype is a stronger determinant of the TME composition than COO.

Considering the significance of the clinical subtype on the expression of immune-related genes, we then compared 80 T-DLBCL samples with 175 DLBCL samples analyzed by mIHC to reveal potential differences in the composition of the TME between T-DLBCL and DLBCL on the cellular level (*Online Supplementary Table S7* and *Online Supplementary Figure S5C*). Compared to DLBCL, the TME of T-DLBCL consisted of a higher proportion of GrB⁺ cytotoxic cells and *CD163*⁺ TAM (median: 0.70% vs. 0.20%; adj. $P < 0.001$ and 12.4% vs. 6.21%; adj. $P = 0.001$, respectively) in particular, whereas the proportion of TIL altogether, T-helper cells, Tregs and *CD163*⁻ TAM was significantly lower (median: 9.78% vs. 14.5%, adj. $P = 0.009$; 5.94% vs. 9.79%, adj. $P < 0.001$; 0.24% vs. 0.85%, adj. $P < 0.001$; and 3.59% vs. 5.84%, adj. $P < 0.001$, respectively) (*Online Supplementary Figure S6A-I*). We also observed that the proportion of different PD-1⁺ cells and LAG3⁺ lymphocytes was lower in T-DLBCL compared to DLBCL (PD-1⁺ cells median: 3.97% vs. 6.26%; adj. $P = 0.015$) (*Online Supplementary Figure S6J-L*). To investigate whether the differences in the composition of the TME between T-DLBCL and DLBCL result from the fact that most T-DLBCL are of ABC origin, we compared the TME composition of GCB and ABC DLBCL separately from GC-type and non-GC-type T-DLBCL. We found only minor differences between the TME of GC and non-GC T-DLBCL (Figure 3B-E and *Online Supplementary Figure S6M-U*). The proportion of some cell types, such as GrB⁺ cells and *CD163*⁺ TAM in GC and non-GC T-DLBCL were comparable with ABC DLBCL, whereas the proportion of other cell types, such as *CD163*⁻ TAM and Tregs were lower in T-DLBCL compared to both GCB and

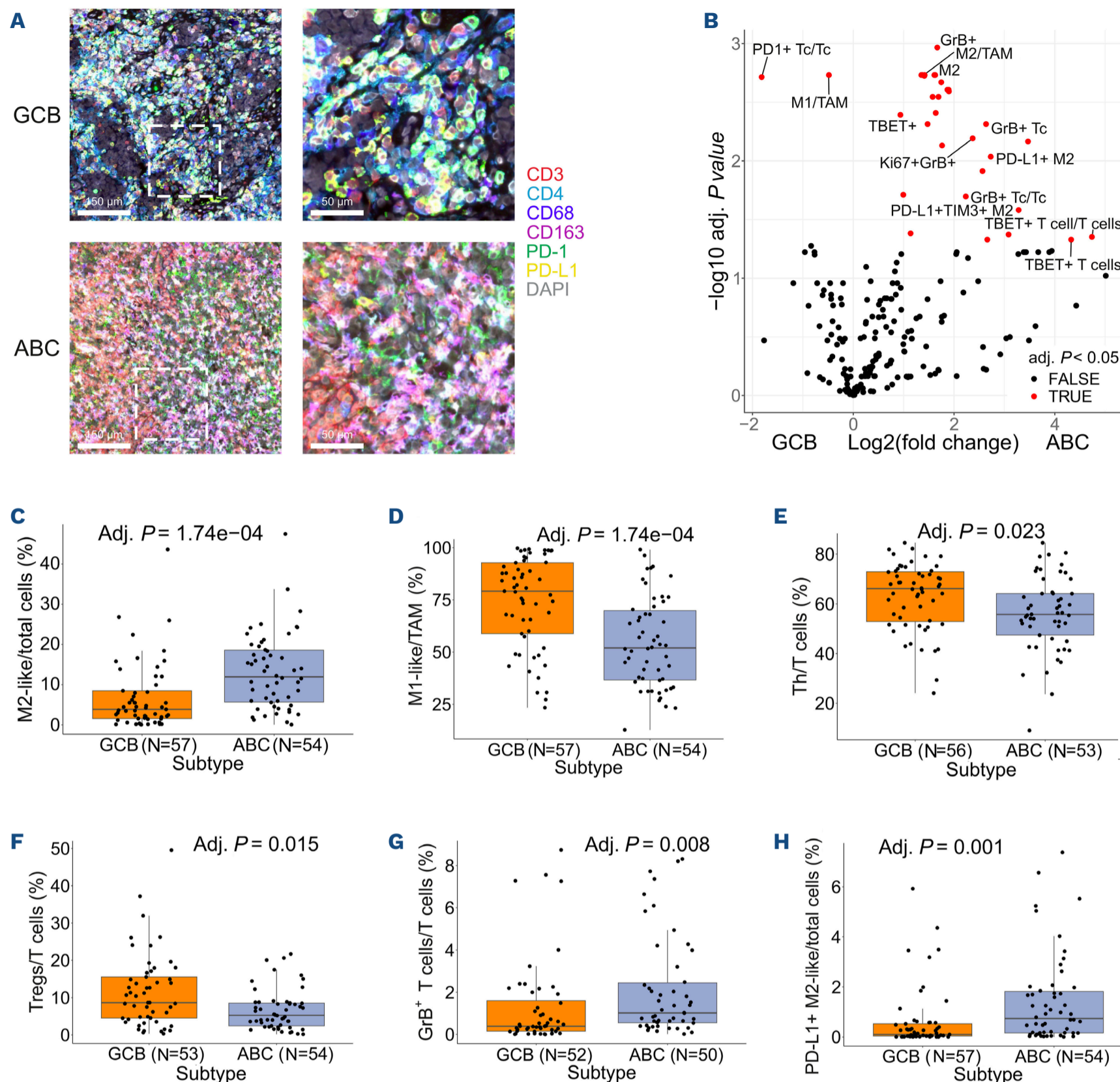


Figure 2. The composition of the tumor microenvironment in germinal center B-cell-like and activated B-cell-like diffuse large B-cell lymphoma analyzed by multiplex immunohistochemistry. (A) Representative images of a germinal center B-cell-like (GCB) and activated B-cell-like (ABC) diffuse large B-cell lymphoma (DLBCL) sample from multiplex immunohistochemistry (mIHC) analyses performed on tissue microarrays (TMA). CD3=red, CD4=cyan, CD68=blue, CD163=magenta, PD-1=green, PD-L1=yellow, DAPI=gray. Scale bars 150 μ m and 50 μ m in the left and right images, respectively. (B) Volcano plot depicting immune cell types whose proportions in the tumor microenvironment (TME) differ most between ABC and GCB DLBCL in the DLBCL, not otherwise specified (NOS), mIHC cohort. Cell proportions indicate proportions of total cells except where stated otherwise. (C-H) Box plots depicting the proportions of M2-like macrophages/total cells (C), M1-like macrophages/macrophages (D), T-helper cells/T cells (E), Regulatory T cells/T cells (F), GrB⁺ T cells/T cells (G), and PD-L1⁺ M2-like macrophages/total cells (H) in the TME of GCB and ABC DLBCL analyzed in the DLBCL, NOS mIHC cohort. Statistical significance was analyzed using the Mann-Whitney U test. Due to staining artefacts, data on certain cell types was unavailable for some samples. TAM=CD68⁺ cells, M2-like=CD163⁺ cells, M1-like=CD163⁺CD68⁺ cells, T cells=CD3⁺ cells, Th=CD4⁺CD3⁺ cells, Tc=CD8⁺ cells, Tregs=FOXP3⁺CD3⁺ cells.

ABC DLBCL (Figure 3B-E and *Online Supplementary Figure S6M-U*). Taken together, the TME of these lymphomas seem to represent a continuum with GCB DLBCL at one end and non-GC T-DLBCL at the other.

Lastly, we analyzed the expression of HLA molecules in T-DLBCL compared to DLBCL. Although the expression of HLA-ABC and B2M was significantly higher in ABC DLBCL compared to GCB DLBCL, the expression of HLA-ABC,

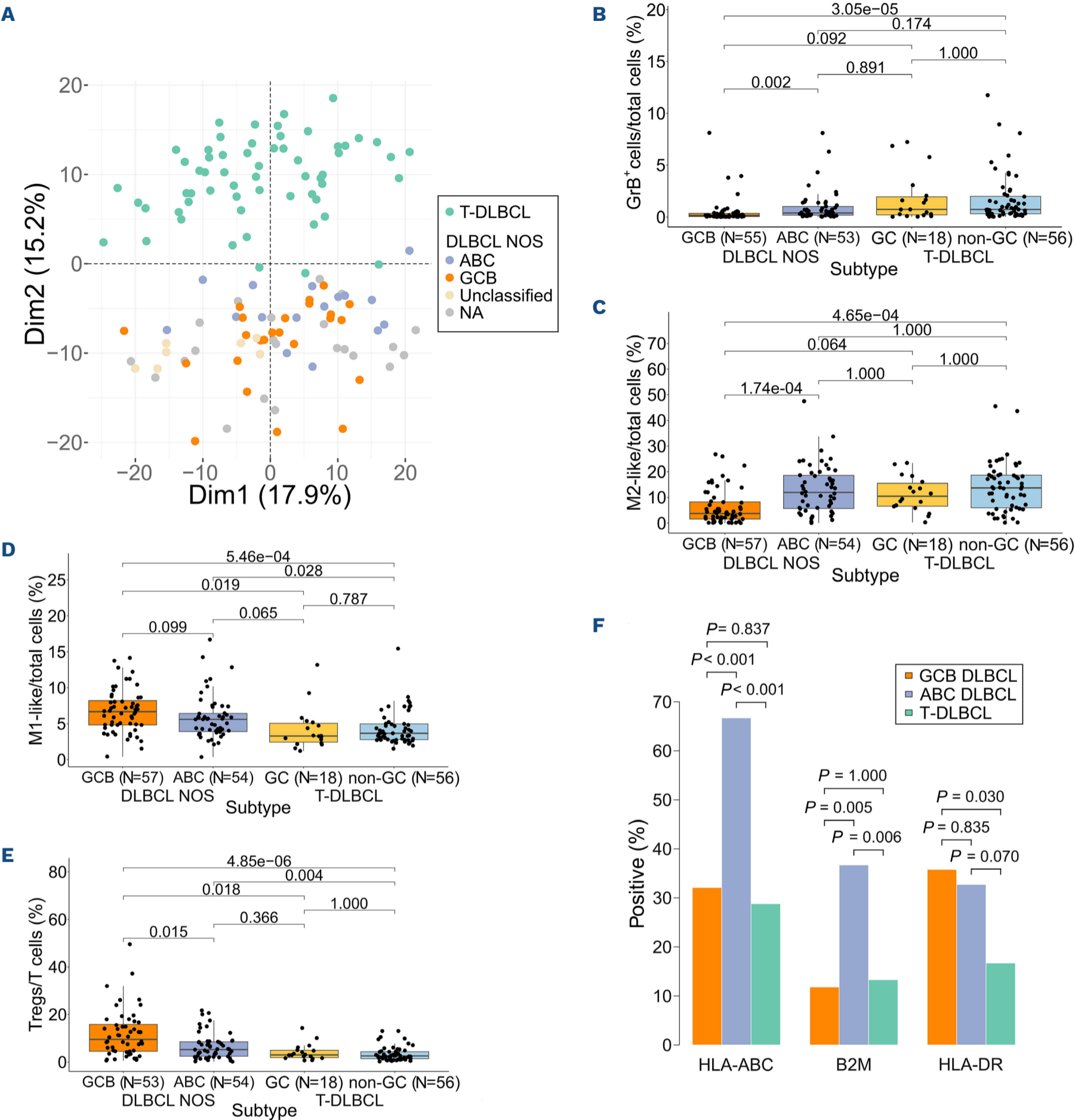


Figure 3. Differently expressed immune-related genes and differences in the constitution of the tumor microenvironment analyzed by multiplex immunohistochemistry between testicular diffuse large B-cell lymphoma and diffuse large B-cell lymphoma, not otherwise specified. (A) Dot plot depicting the first two components of a principal component analysis performed with all available immune-related genes in patients from the testicular diffuse large B-cell lymphoma (T-DLBCL) and the DLBCL, not otherwise specified (DLBCL NOS) gene expression cohorts analyzed by the Nanostring nCounter Human PanCancer Immunoprofiling Panel. (B-E) Box plots depicting the proportions of GrB⁺ cells/total cells (B), M2-like macrophages/total cells (C), M1-like macrophages/total cells (D), and Tregs/T cells (E) in the tumor microenvironment (TME) of germinal center (GC) and non-GC T-DLBCL as well as GCB and activated B-cell like (ABC) DLBCL samples in the T-DLBCL and DLBCL, NOS multiplex immunohistochemistry (mIHC) cohorts. The numbers comparing different subtypes are adjusted (adj.) *P* values for the Mann-Whitney U test comparing the respective groups. Due to staining artefacts, data on certain cell types was unavailable for some samples. (F) Bar plot depicting the proportion of T-DLBCL and GCB and ABC type DLBCL, NOS samples staining positive for HLA-ABC, B2M, and HLA-DR analyzed by IHC in the T-DLBCL and DLBCL, NOS mIHC cohorts. T cells=CD3⁺ cells, Tregs=FOXP3⁺CD4⁺CD3⁺ cells, Tregs/T cells=FOXP3⁺CD3⁺/CD3⁺ cells, M1-like=CD163⁺CD68⁺ cells, M2-like=CD163⁺ cells.

HLA-DR, and B2M was less common in T-DLBCL than in ABC DLBCL (29% vs. 67%, $P<0.001$; 17% vs. 33%, $P=0.070$; and 13% vs. 37%, $P=0.006$, respectively) and expression of HLA-ABC and B2M was comparable to GCB DLBCL (29% vs. 32%, $P=0.837$ and 13% vs. 12%, $P=1.000$) (Figure 3F and *Online Supplementary Figure S6V*).

Differences in cell-to-cell interaction patterns between germinal center B-cell-like, activated B-cell-like, and testicular diffuse large B-cell lymphoma

Next, we wanted to find out whether the differences in the TME composition between GCB and ABC DLBCL were associated with spatial cell-to-cell interactions. When we compared TIL interactions overall, we found that TIL in general and T-helper cells in particular had more interactions with

other TIL and TAM (adj. $P<0.001$ for all) (Figure 4 and *Online Supplementary Figure S7A, B*). In addition, B cells had more interactions with PD-L1⁺ cells in the GCB subtype (Figure 4). In contrast, cytotoxic TIL interacted more often with T-helper cells, cytotoxic T cells, and TAM in general (adj. $P<0.001$, adj. $P=0.003$, and adj. $P=0.017$) (Figure 4 and *Online Supplementary Figure S7A, B*). We did not find any major differences in TAM interactions overall between the subtypes (*Online Supplementary Figure S7A, B*). However, CD163⁺ TAM interacted more often with B cells, TIL, other TAM, and PD-1⁺ cells in the ABC DLBCL compared to GCB DLBCL (adj. $P<0.001$ for all) (Figure 4 and *Online Supplementary Figure S7A, B*). Finally, we studied the interactions of cells expressing immune checkpoint molecules. Notably, we found that PD-1⁺ cells had more interactions with PD-L1⁺ cells and more specifically

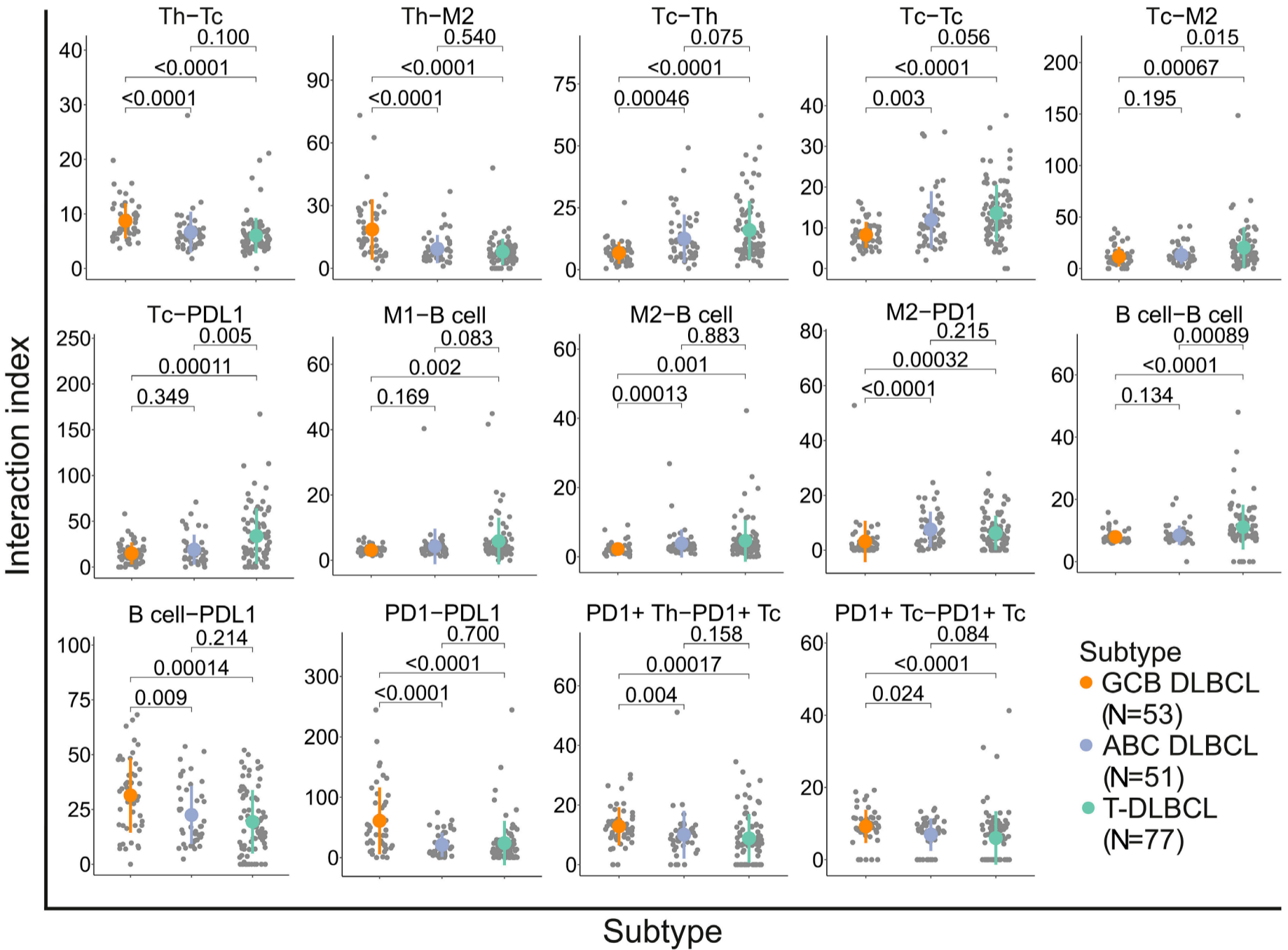


Figure 4. Interactions between different immune cell subtypes in the tumor microenvironment of germinal center B-cell like, activated B-cell-like, and testicular diffuse large B-cell lymphoma. Box plots depicting differences in the number of selected significant interactions between different immune cells in germinal center B-cell-like (GCB) and activated B-cell-like (ABC) diffuse large B-cell lymphoma (DLBCL), not otherwise specified (NOS), and testicular (T)-DLBCL samples in the DLBCL, NOS and T-DLBCL multiplex immunohistochemistry (mIHC) cohorts. Th=CD4⁺CD3⁺ cells, Tc=CD4⁺CD3⁺ cells, M2=CD163⁺ cells, M1=CD163⁺CD68⁺ cells, B cell=CD20⁺ cells, PD1=PD-1⁺ cells, PDL1=PD-L1⁺ cells. *adjusted (adj.) $P<0.05$, **adj. $P<0.01$, ***adj. $P<0.001$, ****adj. $P<0.0001$.

PD-1⁺ T-helper cells and cytotoxic T cells had more interactions with PD-1⁺ T-helper cells in GCB DLBCL compared to ABC DLBCL (adj. *P*<0.001, adj. *P*=0.004, and adj. *P*=0.024) (Figure 4), whereas PD-L1⁺ cells had more interactions with B cells in ABC DLBCL (adj. *P*=0.027) (*Online Supplementary Figure S7A, B*).

In T-DLBCL, cell interactions resembled those in ABC DLBCL. However, there were some differences. Most notably, compared to ABC DLBCL, in T-DLBCL, cytotoxic T cells had more interactions with other TME-associated cells, especially CD163⁺ TAM and PD-L1⁺ cells (adj. *P*=0.015 and adj. *P*=0.005), but also with T-helper cells and other cytotoxic T cells (adj. *P*=0.075 and adj. *P*=0.056). However, statistical significance was not retained after correction for multiple testing (Figure 4). In addition, B cells interacted more often with other B cells in T-DLBCL compared to ABC DLBCL (adj. *P*<0.001) (Figure 4).

Prognostic impact of immune cells and their interactions in the tumor microenvironment of germinal center B-cell-like and activated B-cell-like diffuse large B-cell lymphoma
Beyond studying the differences in the composition of the

TME, we investigated whether the impact of immune cell subtypes on survival differed between the ABC and GCB subtypes and T-DLBCL.^{28,35,40} First, as we have previously reported in DLBCL NOS,¹² the proportion of immune checkpoint-expressing TAM, such as PD-L1 and TIM3 expressing CD163⁺ TAM was associated with poor survival both in GCB and ABC DLBCL (PFS: GCB HR: 2.85, 95% CI: 1.1-7.6, *P*=0.037; ABC HR: 2.92, 95% CI: 1.0-8.1, *P*=0.041) (Figure 5A). In addition to immune checkpoint expressing TAM, TAM altogether, CD163⁺ TAM, and a higher proportion of PD-L1⁺ cells, GrB⁺ cytotoxic immune cells, and TIM3⁺ TIL translated to adverse outcome in GCB but not in ABC DLBCL (PFS HR: 1.24, 95% CI: 1.0-1.5, *P*=0.024; HR: 1.24, 95% CI: 1-06-2.14, *P*=0.021; HR: 1.16, 95% CI: 1.0-1.3, *P*=0.039; HR: 1.51, 95% CI: 1.1-2.1, *P*=0.021, and HR: 1.23, 95% CI: 1.0-1.4, *P*=0.010, respectively) (Figure 5A-D and *Online Supplementary Figure S8A-I*). In contrast, a high proportion of CD8⁺ TIL was associated with better survival in patients with ABC DLBCL, but not in patients with GCB DLBCL (PFS ABC HR: 0.92, 95% CI: 0.84-1.0, *P*=0.048; GCB HR:1.01, 95% CI: 0.89-1.1, *P*=0.888) (Figure 5A and *Online Supplementary Figure S8A, J, K*).

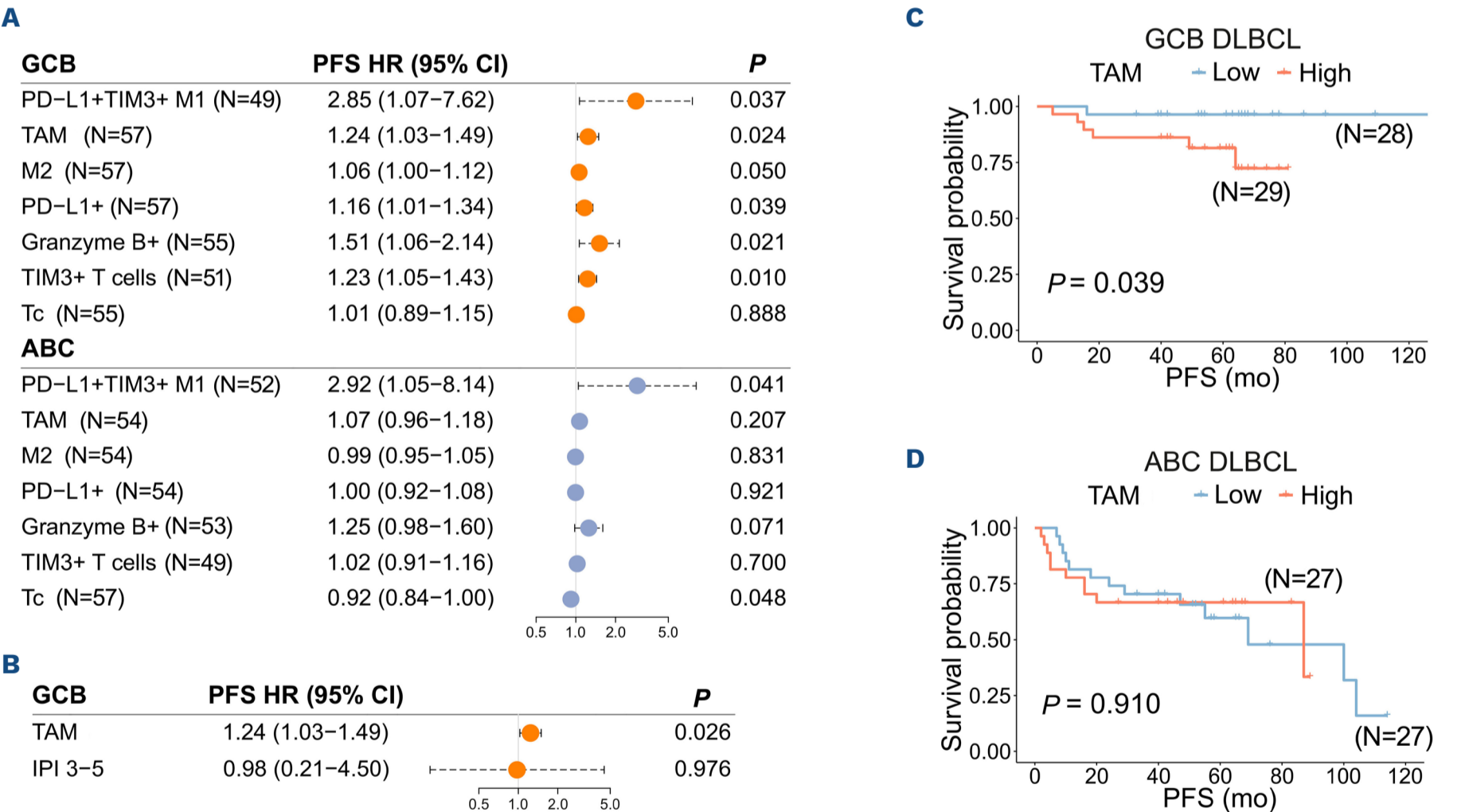


Figure 5. Clinical impact of different immune cells and their interactions in the tumor microenvironment of germinal center B-cell-like, activated B-cell-like, and testicular diffuse large B-cell lymphoma. (A) Forest plot visualizing the impact of selected immune cell subtypes on progression-free survival (PFS) in germinal center B-cell-like (GCB) and activated B-cell-like (ABC) diffuse large B-cell lymphoma (DLBCL) in the DLBCL, not otherwise specified (NOS) multiplex immunohistochemistry (mIHC) cohort, as evaluated by Cox univariable regression analyses with continuous variables. (B) Forest plot visualizing the impact of macrophages on PFS in a Cox multivariable regression analysis with International Prognostic Index (IPI) in patients with GCB DLBCL in the DLBCL, NOS mIHC cohort. (C and D) Kaplan-Meier (log-rank test) survival plots depict PFS in GCB DLBCL (C) and ABC DLBCL (D) patients with high and low proportions of macrophages using median cutoff in the DLBCL, NOS mIHC cohort. TAM=CD68⁺ cells, M1=CD163-CD68⁺ cells, M2=CD163⁺ cells, T cell=CD3⁺ cells, Tc=CD8⁺ cells. mo: months; T-DLBCL: testicular DLBCL; TME: tumor microenvironment.

Finally, we studied the prognostic impact of cell-to-cell interactions. Especially in GCB DLBCL, but also in T-DLBCL, a large number of CD163⁺ TAM interactions with TIL, T-helper cells, and PD-1⁺ cells translated to unfavorable survival (Figure 6A, B and *Online Supplementary Figure S9A-G*). In contrast, CD163⁺ TAM interactions did not impact survival in patients with ABC DLBCL. In addition, in T-DLBCL, a high number of interactions between TIL and TAM, T-helper cells and TAM, and T-helper cells and other TIL was associated with favorable outcomes (Figure 6A, C, D and *Online Supplementary Figure S9H-M*).

Discussion

Previous studies have identified some differences in the TME between the GCB and ABC DLBCL, such as greater cytotoxicity and increased expression of PD-L1 on B cells and macrophages in the ABC subtype.^{10,41} Additionally, certain differences in the

spatial organization between the subtypes have been reported.¹³ A comprehensive comparison of the TME between the GCB and ABC DLBCL has, nevertheless, been missing. In this study, we dissected the composition and spatial organization of the TME in GCB and ABC DLBCL, and T-DLBCL using gene expression profiling and mIHC. We found that ABC DLBCL typically has a more cytotoxic TME, and a predominance of M2-like TAM, whereas the TME in GCB DLBCL is characterized especially by a larger proportion of T-helper cells and Tregs. The TME in T-DLBCL is similar to the TME of ABC DLBCL, which is in line with the fact that T-DLBCL is usually of ABC origin. However, we also observed that the clinical subtype is a stronger determinant of the TME composition than COO. Our cell-to-cell interaction analyses indicated that the cell types over-represented in each subtype are also more involved in the interactions with the other immune cells. Finally, we showed that the differences in the TME composition between the DLBCL subtypes further reflect the differences in the organization of their TME, with different cell types being

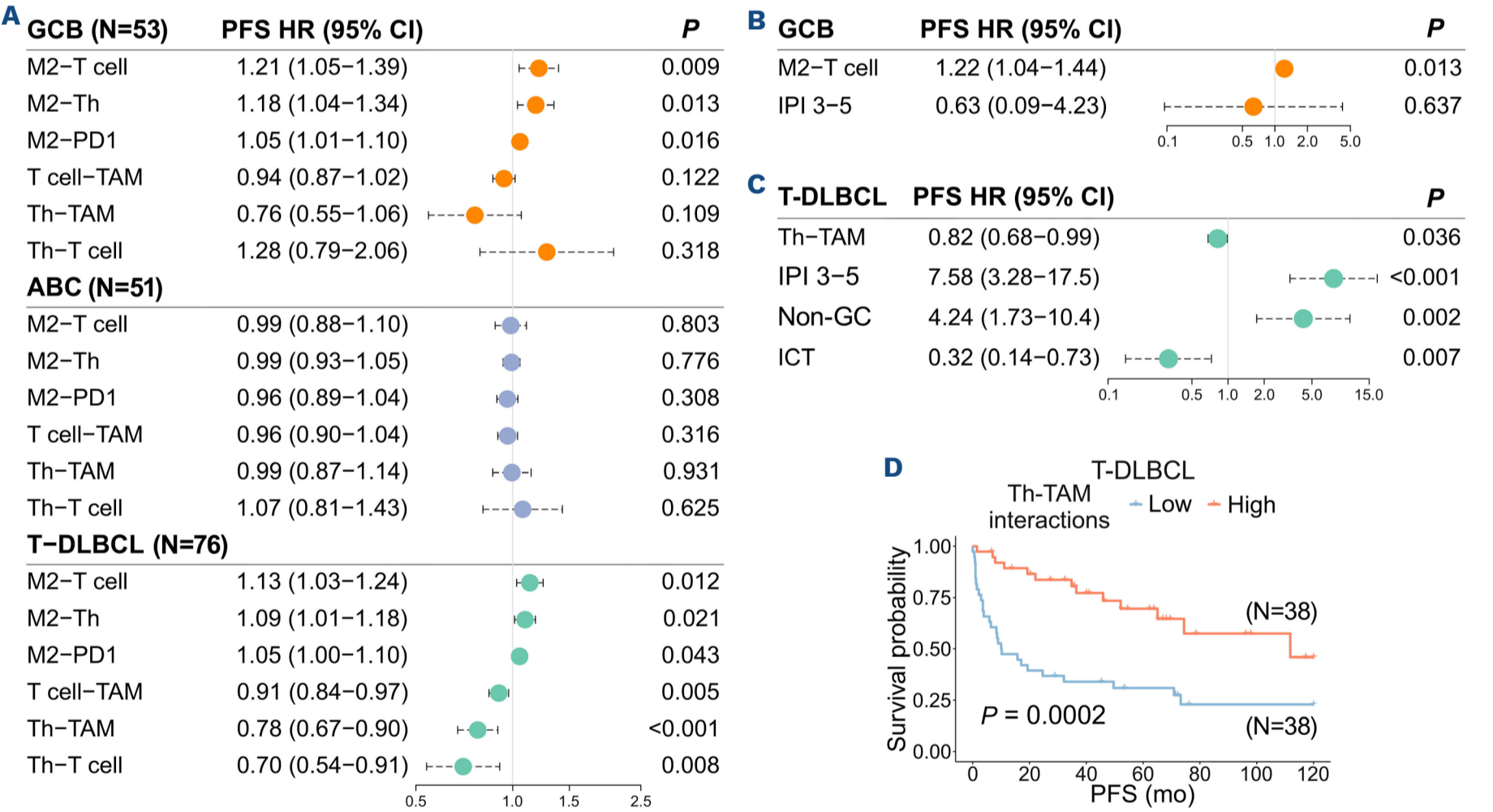


Figure 6. Clinical impact of different immune cell interactions in the tumor microenvironment of germinal center B-cell-like, activated B-cell-like, and testicular diffuse large B-cell lymphoma. (A) Forest plot visualizing the impact of selected immune cell interactions on progression-free survival (PFS) in germinal center B-cell-like (GCB) and activated B-cell-like (ABC) diffuse large B-cell lymphoma (DLBCL) in the DLBCL, not otherwise specified (NOS) multiplex immunohistochemistry (mIHC) cohort, and in testicular (T)-DLBCL in the T-DLBCL mIHC cohort, respectively, as evaluated by Cox univariable regression analyses with continuous variables. (B) Forest plot visualizing the impact of M2-like macrophage-T-cell interactions on PFS in a Cox multivariable regression analysis with International Prognostic Index (IPI) in patients with GCB DLBCL in the DLBCL, NOS mIHC cohort. (C) Forest plot visualizing the impact of T-helper cell-macrophage interactions on PFS in a Cox multivariable regression analysis with IPI, molecular subtype, and treatment (rituximab-containing immunochemotherapy vs. chemotherapy) in patients with T-DLBCL in the T-DLBCL mIHC cohort. (D) Kaplan-Meier (log-rank test) survival plot depicts PFS in T-DLBCL patients with high and low amounts of T-helper cell-macrophage interactions in their tumor microenvironment using median cutoff in the T-DLBCL mIHC cohort. TAM=CD68⁺ cells, M2=CD163⁺ cells, T cell=CD3⁺ cells, Th=CD4⁺CD3⁺ cells, PD1=PD-1⁺ cells. CI: Confidence Interval; HR: hazard Ratio; ICT=immunochemotherapy; mo: months.

clinically meaningful in distinct subtypes.

The TME of T-DLBCL resembled the TME of ABC DLBCL with higher proportions of cytotoxic immune cells and M2-like macrophages and fewer T-helper cells. There were, however, also some differences, most notably the proportions of M1-like macrophages and Tregs. The total number of B cells was also significantly lower in T-DLBCL compared to ABC DLBCL. However, the proportion of most immune cells in T-DLBCL was closer to the proportions in ABC DLBCL than to those in GCB DLBCL. Therefore, it seems that the ABC-type lymphomas shape their TME in T-DLBCL in a similar manner as in ABC DLBCL. Nonetheless, the immune-privileged milieu of the testes most likely has its distinct and unique influence on the entire pathogenesis and the formation of the TME of T-DLBCL, differing somewhat from that of ABC DLBCL. All in all, it appears that, in many cases, the TME in DLBCL and T-DLBCL represent a continuum, with GCB DLBCL and T-DLBCL furthest away from each other, and ABC DLBCL in the middle (Figure 7).

A possible explanation for the different compositions of the TME may be the expression of HLA molecules. We found higher expression of HLA-ABC and B2M in ABC compared to GCB DLBCL, being in line with earlier findings, where MHC-I loss was observed in both GCB (approx. 60%) and ABC (approx. 40%) molecular subtypes.⁴² HLA-ABC molecules present fragments of proteins to cytotoxic cells, which might explain the accumulation of cytotoxic cells in the TME of ABC DLBCL. Previous studies have also found a correlation of HLA molecules with certain immune cell types of the DLBCL TME.²⁸ However, we did not find any direct association between the expression of HLA-ABC and the proportion of cytotoxic cells

or any other major cell type in the TME. Another observation that contradicts the hypothesis of HLA molecules explaining the differences seen in the TME was the finding that T-DLBCL express less frequently HLA molecules than DLBCL NOS, although their TME is rich in cytotoxic cells. Therefore, the expression of HLA molecules is unlikely to be the principal reason behind the differences in the TME.

Previous studies have found multiple different immune cell subtypes correlating with the survival of DLBCL patients^{7-12,43,44}. However, a comparison of the prognostic impact of these cell subtypes and especially their interactions in different DLBCL subtypes has been lacking. We found that the prognostic impact of certain immune cells on survival differed between GCB and ABC DLBCL. Most notably, TAM, PD-L1⁺ cells, GrB⁺ cells, and TIM3⁺ TIL associated with poor survival in GCB DLBCL, whereas, in addition to immune checkpoint expressing TAM, only CD8⁺ TIL correlated positively with outcome in ABC DLBCL. Conversely, we have previously found that the total proportion of TIL, PD-L1⁺ TAM, and PD-1⁺ TIL have a favorable, and TBET⁺FOXP3⁺ Tregs an adverse impact on survival in patients with T-DLBCL.^{28,35,40} The impact these cell types have on survival may be directly related to the different biology of the molecular subtypes. Despite the differences in biology and prognosis, treatment of GCB and ABC DLBCL has remained the same, and TME-directed therapies have so far not been effective.¹⁵ Our findings, nevertheless, raise the question of whether novel TME-targeted therapies could have different efficacy in GCB and ABC DLBCL, as well as in T-DLBCL.

The strengths of our study are the multiple cohorts involved, the availability of both gene expression and immunohisto-

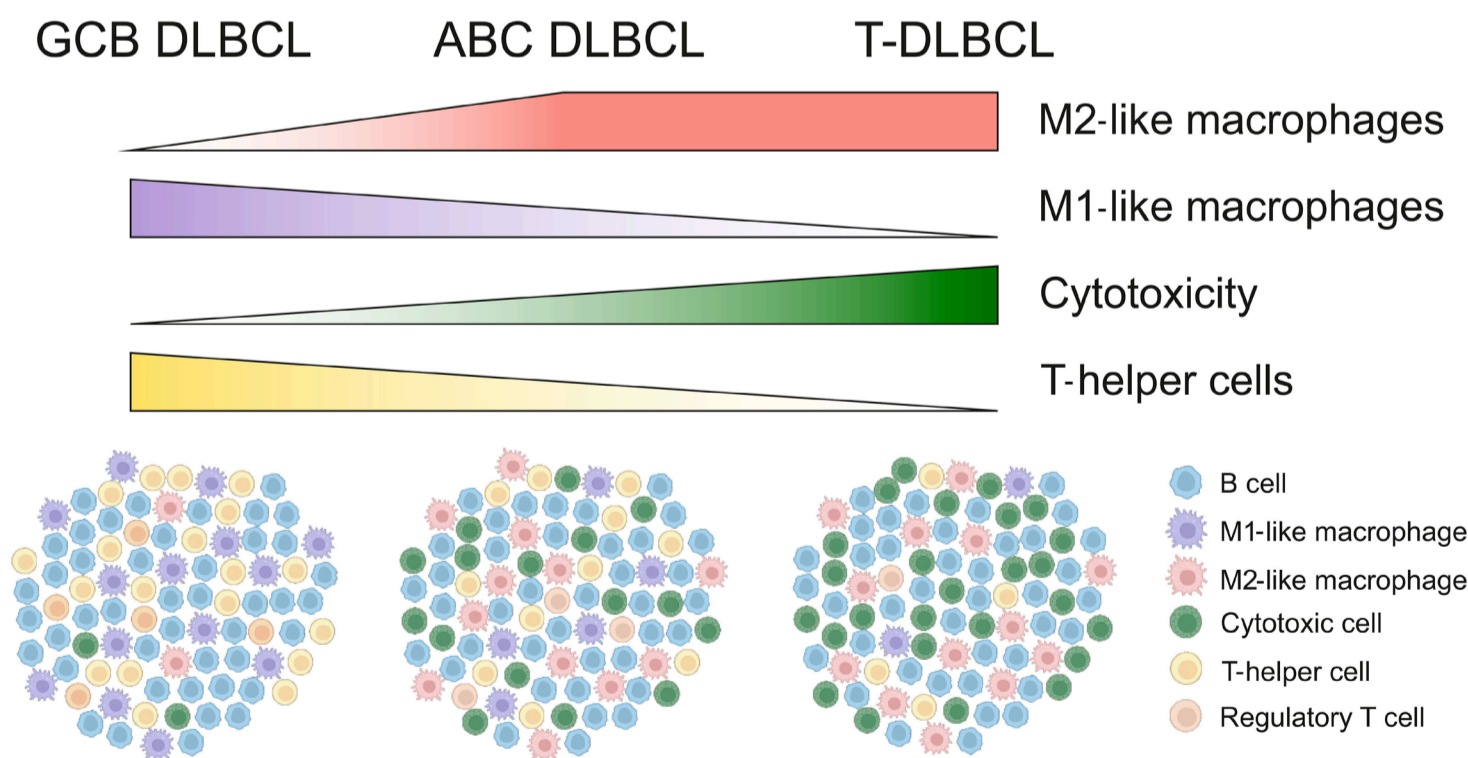


Figure 7. Summary of the differences in the composition of the tumor microenvironment in germinal center B-cell-like and activated B-cell-like diffuse large B-cell lymphoma, diffuse large B-cell lymphoma, not otherwise specified, and testicular diffuse large B-cell lymphoma. Schematic diagram depicting the proportions of M2-like macrophages, M1-like macrophages, cytotoxicity, and T-helper cells in germinal center B-cell-like (GCB) and activated B-cell-like (ABC) diffuse large B-cell lymphoma (DLBCL), DLBCL, not otherwise specified (NOS), and testicular (T)-DLBCL. Images were created using BioRender.com.

chemical data, and the possibility to identify clinically relevant cell-cell interactions. The limitation is that we had only one mIHC cohort available to compare GCB and ABC subtypes. Although the results in two separate gene expression cohorts and ABC-dominated T-DLBCL cohorts further strengthened our observations, validation in a larger mIHC cohort is warranted. In addition, T-DLBCL patients were not uniformly treated, and validation of the prognostic impact of different immune cell subtypes and their interactions in this subtype in another cohort is needed. Furthermore, there were no data on which samples in the DLBCL NOS cohort were nodal and which extranodal. Finally, due to a limited number of samples with genetic information, there was insufficient statistical power to compare the genetic subtypes.

In summary, we have shown in multiple cohorts and overlapping methods that the TME of GCB and ABC DLBCL are distinct. The TME in T-DLBCL resembles the TME of ABC DLBCL. However, clinical subtype is a stronger determinant of the TME composition than COO. Cell-to-cell interaction analyses indicate that the interplay between distinct tumor-infiltrating immune cells also differs according to the subtype. Finally, our data suggest that different TME-targeted therapies might have distinct clinical efficacy based on the DLBCL subtype, although individual differences are undoubtedly also significant.

Disclosures

OB reports consultancy fees from Novartis, Sanofi, GSK, Astellas, and Amgen, all outside the submitted work, research grants from Pfizer and Gilead Sciences, outside the submitted work, and stock ownership of Hematoscope Ltd., outside the submitted work. MP reports consultancy fees from Abbvie, Gilead, Roche, and Sobi, all outside the submitted work, and honoraria from Abbvie, Astra Zeneca, and Gilead. HH reports honoraria and consultancy fees from Incyte, Genmab and Nordic Nanovecto, all outside the submitted work. JMJ reports consultancy fees from Abbvie, Gilead, Roche, Celgene/BMS, Incyte, SOBI, Novartis, and Orion, none of which are related to

this work. SL reports consultancy fees from Abbvie, Genmab, Gilead, Incyte, Novartis, Roche, and Sobi, all outside the submitted work, honoraria from Gilead, Incyte, Novartis, and Sobi, and research grants from Bayer, Celgene/BMS, Hutchmed, Genmab, Novartis, and Roche, all outside the submitted work.

Contributions

MA and S-KL designed and conceived the study, analyzed data, and wrote the manuscript. OB performed cell interaction analyses. MP designed the study and participated in data analysis. M-LK-L, KB, JMJ and HH provided samples. TP designed and performed mIHC data analyses. SL designed and supervised the study, and wrote the manuscript. All authors revised and approved the final manuscript for publication.

Acknowledgments

We thank Annabrita Schoonenberg (FIMM) and the Digital and Molecular Pathology Unit supported by Helsinki University and Biocenter Finland for performing the mIHC stainings, Anne Aarnio for technical assistance, and biorender.com for support in designing Figure 7.

Funding

This research was funded by grants from the Research Council of Finland (to SL), Finnish Cancer Organizations (to SL), Sigrid Juselius Foundation (to SL), University of Helsinki (to SL), Helsinki University Hospital (to SL), iCAN Digital Precision Cancer Medicine Flagship (to SL), Biomedicum Helsinki Foundation (to MA), Finnish Society of Oncology (to MA), Finska Läkaresällskapet (to MA), the Finnish Medical Foundation (to MP), the Maud Kuistila Memorial Foundation (to MP), and the Relander Foundation (to MP). Open access funded by Helsinki University Library.

Data-availability statement

Data are available from the corresponding author upon reasonable request.

References

1. Scott DW, Gascoyne RD. The tumour microenvironment in B cell lymphomas. *Nat Rev Cancer*. 2014;14(8):517-534.
2. Nicholas NS, Apollonio B, Ramsay AG. Tumor microenvironment (TME)-driven immune suppression in B cell malignancy. *Biochim Biophys Acta*. 2016;1863(3):471-482.
3. Gajewski TF, Schreiber H, Fu YX. Innate and adaptive immune cells in the tumor microenvironment. *Nat Immunol*. 2013;14(10):1014-1022.
4. Kotlov N, Bagaev A, Revuelta MV, et al. Clinical and biological subtypes of B-cell lymphoma revealed by microenvironmental signatures. *Cancer Discov*. 2021;11(6):1468-1489.
5. Steen CB, Luca BA, Esfahani MS, et al. The landscape of tumor cell states and ecosystems in diffuse large B cell lymphoma. *Cancer Cell*. 2021;39(10):1422-1437.e10.
6. Fridman WH, Pages F, Sautes-Fridman C, Galon J. The immune contexture in human tumours: impact on clinical outcome. *Nat Rev Cancer*. 2012;12(4):298-306.
7. Cai QC, Liao H, Lin SX, et al. High expression of tumor-infiltrating macrophages correlates with poor prognosis in patients with diffuse large B-cell lymphoma. *Med Oncol*. 2012;29(4):2317-2322.
8. Keane C, Gill D, Vari F, Cross D, Griffiths L, Gandhi M. CD4(+) tumor infiltrating lymphocytes are prognostic and independent of R-IPi in patients with DLBCL receiving R-CHOP chemotherapy. *Am J Hematol*. 2013;88(4):273-276.
9. Riihijärvi S, Fiskvik I, Taskinen M, et al. Prognostic influence of macrophages in patients with diffuse large B-cell lymphoma: a correlative study from a Nordic phase II trial. *Haematologica*. 2015;100(2):238-245.
10. Xu-Monette ZY, Xiao M, Au Q, et al. Immune profiling and

- quantitative analysis decipher the clinical role of immune-checkpoint expression in the tumor immune microenvironment of DLBCL. *Cancer Immunol Res.* 2019;7(4):644-657.
11. Autio M, Leivonen SK, Brück O, et al. Immune cell constitution in the tumor microenvironment predicts the outcome in diffuse large B-cell lymphoma. *Haematologica.* 2021;106(3):718-729.
 12. Autio M, Leivonen SK, Brück O, Karjalainen-Lindsberg ML, Pellinen T, Leppä S. Clinical impact of immune cells and their spatial interactions in diffuse large B-cell lymphoma microenvironment. *Clin Cancer Res.* 2022;28(4):781-792.
 13. Colombo AR, Hav M, Singh M, et al. Single-cell spatial analysis of tumor immune architecture in diffuse large B-cell lymphoma. *Blood Adv.* 2022;6(16):4675-4690.
 14. Wright KT, Weirather JL, Jiang S, et al. Diffuse large B-cell lymphomas have spatially defined, tumor immune microenvironments revealed by high-parameter imaging. *Blood Adv.* 2023;7(16):4633-4646.
 15. Ansell SM, Minnema MC, Johnson P, et al. Nivolumab for relapsed/refractory diffuse large B-cell lymphoma in patients ineligible for or having failed autologous transplantation: a single-arm, phase II study. *J Clin Oncol.* 2019;37(6):481-489.
 16. Alizadeh AA, Eisen MB, Davis RE, et al. Distinct types of diffuse large B-cell lymphoma identified by gene expression profiling. *Nature.* 2000;403(6769):503-511.
 17. Fu K, Weisenburger DD, Choi WW, et al. Addition of rituximab to standard chemotherapy improves the survival of both the germinal center B-cell-like and non-germinal center B-cell-like subtypes of diffuse large B-cell lymphoma. *J Clin Oncol.* 2008;26(28):4587-4594.
 18. Lenz G, Wright G, Dave SS, et al. Stromal gene signatures in large-B-cell lymphomas. *N Engl J Med.* 2008;359(22):2313-2323.
 19. Bea S, Zettl A, Wright G, et al. Diffuse large B-cell lymphoma subgroups have distinct genetic profiles that influence tumor biology and improve gene-expression-based survival prediction. *Blood.* 2005;106(9):3183-3190.
 20. Pasqualucci L, Dalla-Favera R. Genetics of diffuse large B-cell lymphoma. *Blood.* 2018;131(21):2307-2319.
 21. Davis RE, Brown KD, Siebenlist U, Staudt LM. Constitutive nuclear factor kappaB activity is required for survival of activated B cell-like diffuse large B cell lymphoma cells. *J Exp Med.* 2001;194(12):1861-1874.
 22. Morin RD, Johnson NA, Severson TM, et al. Somatic mutations altering EZH2 (Tyr641) in follicular and diffuse large B-cell lymphomas of germinal-center origin. *Nat Genet.* 2010;42(2):181-185.
 23. Rosenwald A, Wright G, Chan WC, et al. The use of molecular profiling to predict survival after chemotherapy for diffuse large-B-cell lymphoma. *N Engl J Med.* 2002;346(25):1937-1947.
 24. Schmitz R, Wright GW, Huang DW, et al. Genetics and pathogenesis of diffuse large B-cell lymphoma. *N Engl J Med.* 2018;378(15):1396-1407.
 25. Chapuy B, Stewart C, Dunford AJ, et al. Molecular subtypes of diffuse large B cell lymphoma are associated with distinct pathogenic mechanisms and outcomes. *Nat Med.* 2018;24(5):679-690.
 26. Cheah CY, Wirth A, Seymour JF. Primary testicular lymphoma. *Blood.* 2014;123(4):486-493.
 27. Deng L, Xu-Monette ZY, Lohgavi S, et al. Primary testicular diffuse large B-cell lymphoma displays distinct clinical and biological features for treatment failure in rituximab era: a report from the International PTL Consortium. *Leukemia.* 2016;30(2):361-372.
 28. Leivonen SK, Pollari M, Bruck O, et al. T-cell inflamed tumor microenvironment predicts favorable prognosis in primary testicular lymphoma. *Haematologica.* 2019;104(2):338-346.
 29. Holte H, Leppä S, Björkholm M, et al. Dose-densified chemoimmunotherapy followed by systemic central nervous system prophylaxis for younger high-risk diffuse large B-cell/follicular grade 3 lymphoma patients: results of a phase II Nordic Lymphoma Group study. *Ann Oncol.* 2013;24(5):1385-1392.
 30. Leppä S, Jørgensen J, Tierens A, et al. Patients with high-risk DLBCL benefit from dose-dense immunochemotherapy combined with early systemic CNS prophylaxis. *Blood Adv.* 2020;4(9):1906-1915.
 31. Meriranta L, Pasanen A, Alkods A, Haukka J, Karjalainen-Lindsberg ML, Leppä S. Molecular background delineates outcome of double protein expressor diffuse large B-cell lymphoma. *Blood Adv.* 2020;4(15):3742-3753.
 32. Reddy A, Zhang J, Davis NS, et al. Genetic and functional drivers of diffuse large B cell lymphoma. *Cell.* 2017;171(2):481-494.e415.
 33. Scott DW, Wright GW, Williams PM, et al. Determining cell-of-origin subtypes of diffuse large B-cell lymphoma using gene expression in formalin-fixed paraffin-embedded tissue. *Blood.* 2014;123(8):1214-1217.
 34. Isaksen KT, Beiske K, Smeland EB, et al. The DLBCL90 gene-expression assay identifies double-hit lymphomas with high sensitivity in patients from two phase II clinical trials with high-risk diffuse large B-cell lymphoma. *EJHaem.* 2021;2(1):104-108.
 35. Pollari M, Pellinen T, Karjalainen-Lindsberg ML, Kellokumpu-Lehtinen PL, Leivonen SK, Leppä S. Adverse prognostic impact of regulatory T-cells in testicular diffuse large B-cell lymphoma. *Eur J Haematol.* 2020;105(6):712-721.
 36. Berg S, Kutra D, Kroeger T, et al. ilastik: interactive machine learning for (bio)image analysis. *Nat Methods.* 2019;16(12):1226-1232.
 37. Carpenter AE, Jones TR, Lamprecht MR, et al. CellProfiler: image analysis software for identifying and quantifying cell phenotypes. *Genome Biol.* 2006;7(10):R100.
 38. Brück O, Lee MH, Turkkilä R, et al. Spatial immunoprofiling of the intratumoral and peritumoral tissue of renal cell carcinoma patients. *Mod Pathol.* 2021;34(12):2229-2241.
 39. Liarski VM, Sibley A, van Panhuys N, et al. Quantifying in situ adaptive immune cell cognate interactions in humans. *Nat Immunol.* 2019;20(4):503-513.
 40. Pollari M, Bruck O, Pellinen T, et al. PD-L1(+) tumor-associated macrophages and PD-1(+) tumor-infiltrating lymphocytes predict survival in primary testicular lymphoma. *Haematologica.* 2018;103(11):1908-1914.
 41. Dufva O, Pölönen P, Brück O, et al. Immunogenomic landscape of hematological malignancies. *Cancer Cell.* 2020;38(3):380-399.e313.
 42. Fangazio M, Ladewig E, Gomez K, et al. Genetic mechanisms of HLA-I loss and immune escape in diffuse large B cell lymphoma. *Proc Natl Acad Sci U S A.* 2021;118(22):e2104504118.
 43. McCord R, Bolen CR, Koeppen H, et al. PD-L1 and tumor-associated macrophages in de novo DLBCL. *Blood Adv.* 2019;3(4):531-540.
 44. Li L, Sun R, Miao Y, et al. PD-1/PD-L1 expression and interaction by automated quantitative immunofluorescent analysis show adverse prognostic impact in patients with diffuse large B-cell lymphoma having T-cell infiltration: a study from the International DLBCL Consortium Program. *Mod Pathol.* 2019;32(6):741-754.